

CFD Simulations to Validate Two & Three Phase Up-flow in Bubble Columns

Shyam Kumar, Nannuri Srinivasulu and Ashok Khanna

Abstract—Bubble columns have a variety of applications in absorption, bio-reactions, catalytic slurry reactions, and coal liquefaction; because they are simple to operate, provide good heat and mass transfer, having less operational cost. The use of Computational Fluid Dynamics (CFD) for bubble column becomes important, since it can describe the fluid hydrodynamics on both local and global scale. Euler- Euler two-phase fluid model has been used to simulate two-phase (air and water) transient up-flow in bubble column (15cm diameter) using FLUENT6.3. These simulations and experiments were operated over a range of superficial gas velocities in the bubbly flow and churn turbulent regime (1 to 16 cm/s) at ambient conditions. Liquid velocity was varied from 0 to 16cm/s. The turbulence in the liquid phase is described using the standard $k-\epsilon$ model. The interactions between the two phases are described through drag coefficient formulations (Schiller Neumann). The objectives are to validate CFD simulations with experimental data, and to obtain grid-independent numerical solutions. Quantitatively good agreements are obtained between experimental data for hold-up and simulation values. Axial liquid velocity profiles and gas holdup profiles were also obtained for the simulation.

Keywords—Bubble column, Computational fluid dynamics, Gas holdup profile, $k-\epsilon$ model.

I. INTRODUCTION

MULTIPHASE flow processes are important for several reactor technologies. The presence of more than one phase makes the bubble column complex in design and scale up [1]. Bubble columns serve as multiphase contactors and reactors in the chemical, petro-chemical, biochemical, and metallurgical industries, primarily because of the ease and low cost of construction, simplicity of operation, ability to handle solids, excellent heat and mass transfer characteristics, and no sealing problems due to the absence of mechanically moving parts [2]. In spite of the simplicity in mechanical design, fundamental behavior of dynamics of a bubble column reactor is still not fully understood because of the complex nature of multiphase flow [1]. Numerous design parameters (sparger design, reactor geometry) and operating variables (gas flow rate, liquid flow rate, pressure, solid concentration), affect the highly interactive phenomena in slurry bubble column reactor and its performance [3]-[6]. Because of the above facts,

bubble columns have been the object of much attention during these last 25 years; it has also become a benchmarking reactor for both advanced measuring techniques and CFD.

II. EXPERIMENTAL DETAILS

The column is constructed from Plexi-glass. For ease of installation and removal for cleaning purpose, the column was divided into three sections, each of 64 cm and attached through flanges. The ID of column is 15 cm, and wall thickness is 5 mm. The total height of column is 2.72 m. A gas disengagement section is provided at the top of column. The gas phase enters from bottom through a gas distributor. Liquid phase enters the column through a conical section at the bottom of the column. A distributor plate is provided for uniform distribution of liquid phase. Taps are provided at different axial location to measure the pressure drop in the column through DPT's. Liquid flows through a 3.75 cm pipe line, which can sustain a maximum pressure of 1.5 MPa. An outlet of 5 cm is provided at the top for the disengagement of gas and liquid/slurry phase, and finally the liquid/slurry flows back to a storage tank. Air flows through a 1.25 cm SS pipeline. Compressed atmospheric air is used as gas phase, while tap water is used as liquid phase. The Differential Pressure Transducer (DPT) measures the pressure difference and transmits an output signal proportional to the measured variable over a 4 to 20 milli-ampere current. Data Acquisition card (DAQ card), PCI-6024E (National Instruments) has been installed in an Intel PC for collecting the data from the DPT's. LABVIEW is used for collecting the analog input from the DAQ card, converting into digital output and storing the data. Pressure measurements have always been carried out at a frequency of 50 Hz with a total acquisition length of 10000 points (200 s) for each measurement.

III. COMPUTATIONAL MODELS

A. Different models

The use of computational fluid dynamics (CFD) for bubble column is important since it can predict and describe the fluid hydrodynamics on both local and global scale. Two main approaches are often used when modeling gas-liquid flow in bubble columns: Euler-Euler (E-E) [7-13] and Euler-Lagrange (E-L) [14-17]. The E-E approach (the two-fluid model) considers the gas and liquid phases in an Eulerian representation as two interpenetrating fluids. The phases interact through the inter-phase transfer terms and individual solutions of the mass and momentum balances are needed [18]. On the other hand, the E-L approach tracks each bubble

Shyam Kumar is in the dept. of Chemical Engineering at Indian Institute of Technology, Kanpur-208016, India (phone: +91512-2597852; e-mail: shyamk@iitk.ac.in).

Nannuri Srinivasulu has completed his M.Tech in the dept. of Chemical Engineering at Indian Institute of Technology, Kanpur-208016, India (phone: +91512-2597512; e-mail: vasunannuri@gmail.com).

Ashok Khanna, is a prof in the dept. of Chemical Engineering at Indian Institute of Technology, Kanpur-208016, India (phone: +91512-2597117; e-mail: akhanna@iitk.ac.in).

separately while the liquid phase is treated as a continuum. In this way, separate force balance equations are solved for each individual bubble while both phases interact through a source term in the momentum equation. The use of the E-L model allows the introduction of coalescence, break-up and collisions relatively easy, but the number of bubbles is limited and it is computationally expensive. Additionally, E-E simulations are applicable to a wider range of volume fractions, while E-L is restricted to low particle volume fractions as the fraction of volume taken by the particles is not included in the continuous phase calculation. Furthermore, the use of high order discretization schemes with the E-E approach solve the problem of the higher numerical diffusion obtained in comparison with the E-L approach, a fact described by Sokolichin et al. [19]. In this present work E-E approach is adapted. All the simulations are done using Fluent 6.3.

B. Euler-Euler model

Here continuity and momentum equations for each phase need to be solved. The continuity equation is given by

$$\sum_{\alpha=1}^{N_p} \varepsilon_{\alpha} = 1 \quad (1)$$

$$\frac{\partial}{\partial t} \varepsilon_{\alpha} \rho_{\alpha} + \nabla \cdot (\varepsilon_{\alpha} (\rho_{\alpha} U_{\alpha})) = 0 \quad (2)$$

The momentum equation is given by

$$\frac{\partial}{\partial t} \varepsilon_{\alpha} \rho_{\alpha} U_{\alpha} + \nabla \cdot (\varepsilon_{\alpha} (\rho_{\alpha} U_{\alpha} U_{\alpha} - \mu_{\alpha} (\nabla U_{\alpha} + (\nabla U_{\alpha})^T))) = \varepsilon_{\alpha} (\rho g - \nabla p_{\alpha}) + \sum_{\beta=1}^{N_p} c_{\alpha\beta}^{(d)} (\rho_{\beta} U_{\beta} - U_{\alpha}) \quad (3)$$

C. Turbulence models

The equation for turbulent kinetic energy (k) is described as

$$\frac{\partial}{\partial t} (\rho_{\alpha} \varepsilon_{\alpha} k) + \nabla \cdot (\rho_{\alpha} \varepsilon_{\alpha} \bar{v}_{\beta} k) = -\nabla \cdot \left(\frac{\mu_t}{\sigma_k} \nabla k \right) + \varepsilon_{\alpha} (G - \rho_{\alpha} \varepsilon) \quad (4)$$

while the equation for dissipation rate (ε) is

$$\frac{\partial}{\partial t} (\rho_{\alpha} \varepsilon_{\alpha} \varepsilon) + \nabla \cdot (\rho_{\alpha} \varepsilon_{\alpha} \bar{v}_{\beta} \varepsilon) = -\nabla \cdot \left(\frac{\mu_t}{\sigma_{\varepsilon}} \nabla \varepsilon \right) + \varepsilon_{\alpha} (C_1 G - C_2 \rho_{\alpha} \varepsilon) \quad (5)$$

The term G in the in both turbulent kinetic energy (k) and turbulent dissipation rate (ε) equations is defined as $G = \tau_{\alpha} : \nabla \bar{v}_{\alpha}$

The turbulent viscosity, μ_t is computed by combining k and ε as follows:

$$\mu_t = \rho C_{\mu} \frac{k^2}{\varepsilon} \quad (6)$$

The model constants for Standard k - ε turbulence model are $C_{\mu} = 0.09$; $\sigma_k = 1$; $\sigma_{\varepsilon} = 1.3$; $C_1 = 1.44$; $C_2 = 1.92$.

D. Simulation Methodology

Initial and Boundary Conditions:

The simulation domain is between the sparger and the top of the column. We have used the correlation given by Mandelson [20] to calculate the terminal rise velocity

$$V_t = \sqrt{\frac{\sigma}{r_b \rho_l} + g r_b} \quad (7)$$

Here r_b is the radius of the bubble, σ is the surface tension of liquid phase, ρ_l is the density of the liquid phase and g is acceleration due to gravity. Gas holdup, Turbulent kinetic energy and dissipation rate at the inlet is calculated using the following equations:

$$\varepsilon_g = \frac{U_g}{V_t + \frac{U_g}{1 - \varepsilon_g}} \quad (8)$$

Turbulent kinetic energy is given by,

$$k_{in} = 0.004 * U_{l,in}^2 \quad (9)$$

Turbulent dissipation rate is given by,

$$\varepsilon_{in} = C_{\mu}^{3/4} * k_{in}^{3/2} / (0.07D) \quad (10)$$

where, D is the diameter of the column and C_{μ} is a constant and is equal to 0.09.

Initially the column was assumed to be completely filled with water. Inlet variable values were specified based on the mode of flow - batch or co-current. Gas phase inlet velocity has been specified as the terminal rise velocity for batch column. No slip condition was applied at all the walls. Outlet has been defined as pressure outlet and inlet as velocity inlet. 10% of the inlet was assumed as wall to match the actual sparger geometry. For all simulations, a time step was of 0.01 seconds was used with total flow time of 100 seconds. SIMPLEC technique has been used for pressure-velocity coupling [21]. The under relaxation values for pressure and momentum equation were set to 0.6 and 0.4 respectively. First order upwind scheme has been used for discretization of differential equations. For co-current flow of both the phases, the same technique applied for batch case has been applied. However in this simulation, at $t = 0$ sec, the column was assumed to be empty, and both the phases were allowed to enter the column. Schiller-Naumann [22]; Zhang and Vanderheyden [23]; and Tomiyama [24] drag force models have been used for present work.

IV. RESULTS AND DISCUSSION

A. Two Phase Simulation

In the present work, CFD simulations were done using different bubble sizes in the range 4-7mm. Schiller Naumann drag model has been used for the simulations. The predicted results for gas holdup have been presented in Table I along with RMSD values. The predicted gas holdup profile with 5 mm bubble size shows good match with experimental results as shown in the Fig. 1. Therefore, a constant bubble size of 5mm has been used for remaining simulations.

TABLE I
AVERAGE GAS HOLDUP FOR DIFFERENT BUBBLE SIZE

U _g , Cm/s	Average Gas Holdup				
	Experiment	Simulation			
		4 mm	5 mm	6 mm	7 mm
1.13	0.0169	0.0222	0.0203	0.0182	0.0176
2.26	0.0324	0.0422	0.039	0.0363	0.0342
3.4	0.0463	0.0607	0.0564	0.0529	0.05
4.53	0.0616	0.0773	0.0724	0.0682	0.0647
5.66	0.076	0.0924	0.0879	0.0825	0.0786
6.79	0.1036	0.1076	0.1051	0.0958	0.0916
7.93	0.1258	0.1234	0.1221	0.1087	0.1037
9.06	0.1477	0.1387	0.1406	0.1232	0.1157
10.19	0.1677	0.1574	0.1617	0.1384	0.1288
11.32	0.1857	0.184	0.1792	0.1527	0.1414
12.46	0.2003	0.2242	0.2094	0.1813	0.1578
13.59	0.2137	0.247	0.2226	0.2065	0.1848
14.72	0.2269	0.2683	0.2345	0.2242	0.212
16.28	0.2447	0.3046	0.2538	0.2514	0.2294
	RMSD	0.0239	0.0078	0.0158	0.0243

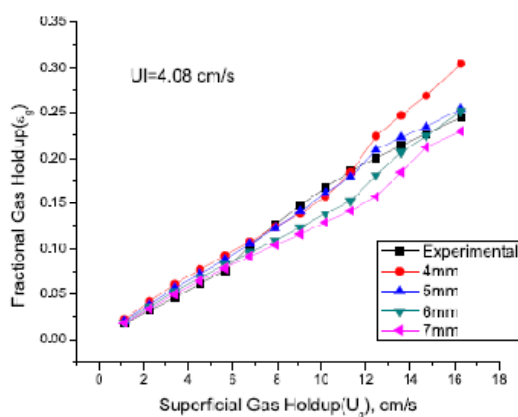


Fig. 1 Effect of bubble diameter over gas holdup

To see the effect of drag laws, a comparative study of these three models has been shown in the Fig. 2. Out of these models Schiller Naumann drag law shows a better agreement with the experimental calculations.

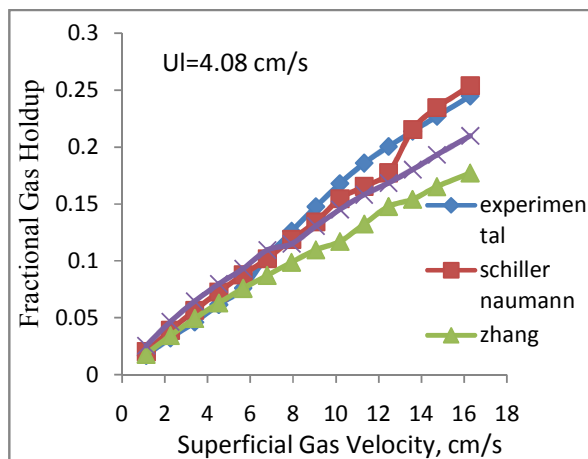


Fig. 2 Comparison of fractional gas holdup calculated by different drag models with experimental value

Fig. 3 shows a comparison for average gas holdup. Experimental values have been calculated by measuring the pressure fluctuations using DPTs, while simulation values have been obtained using the method described above. Fig. 3 (a) to (c) show a good agreement between the experimental and simulation values for liquid velocities up to 12.16 cm/s. After this velocity, the differences between the two values are much larger, where simulation values are always higher than the experimental values. Since the constant bubble size of 5 mm is valid only for low liquid velocities, Hence simulation beyond 12 cm/s doesn't match well with experimental data. We need to incorporate bubble break-up and coalescence for those simulations.

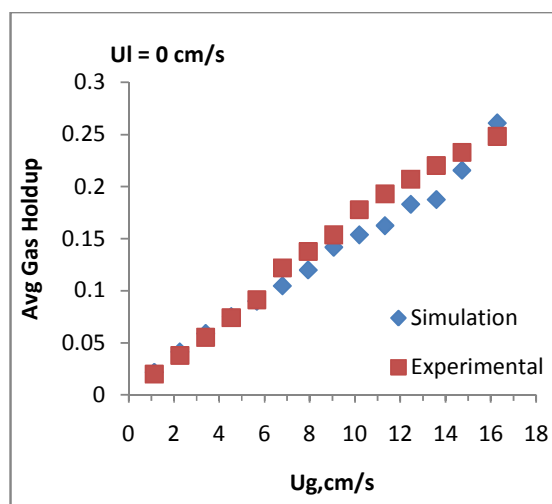


Fig. 3 (a) Comparison between experimental and simulated average gas holdup values for $U_l = 0$ cm/s

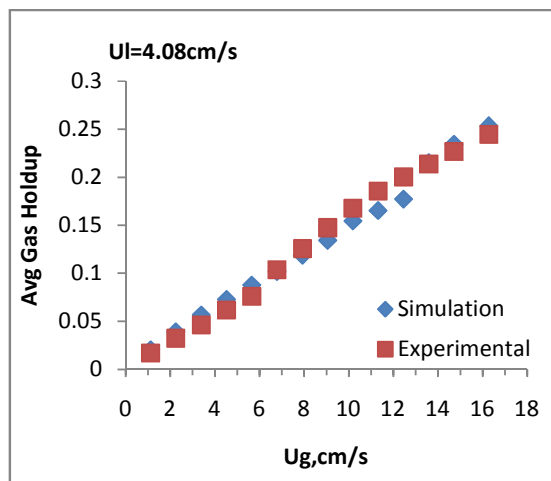


Fig. 3 (b) Comparison between experimental and simulated average gas holdup values for $U_l = 4.08$ cm/s

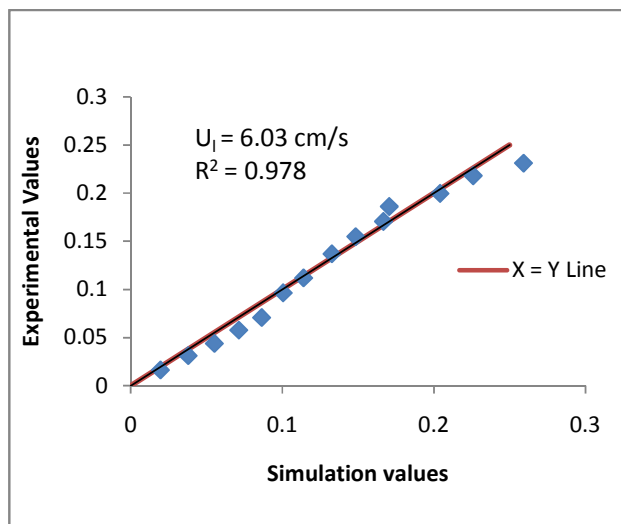


Fig. 4 Comparison of Experimental and Simulated gas holdup

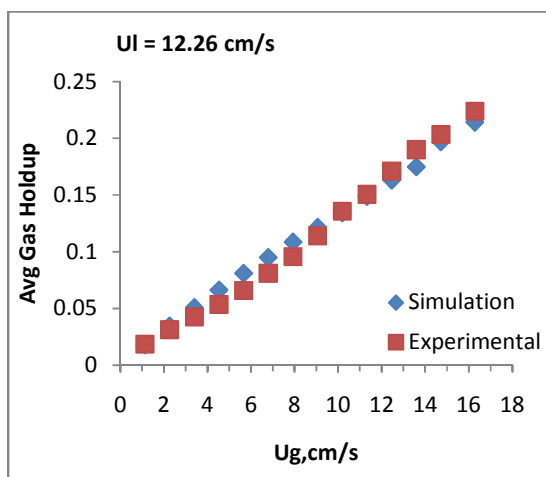


Fig. 3 (c) Comparison between experimental and simulated average gas holdup values for $U_l = 12.26$ cm/s

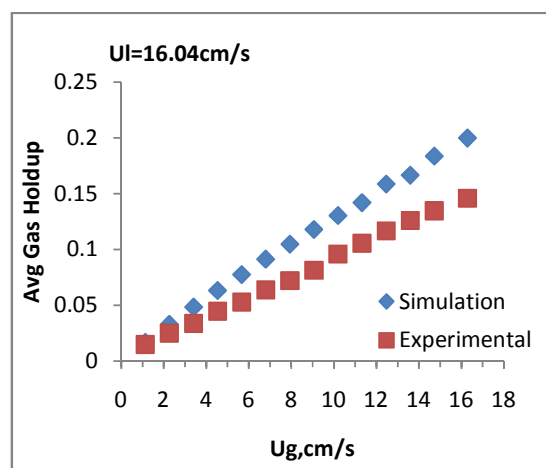


Fig. 3 (d) Comparison between experimental and simulated average gas holdup values for $U_l = 16.04$ cm/s

Fig. 4 compares the experimental gas holdup with the simulated values. The R^2 for the linear fit is 0.978. Thus the simulation is reasonably able to predict the average gas holdup values. In the axial liquid velocity profiles (Fig. 5), a cross over point can be observed where the axial velocity becomes zero. As the liquid velocity increases, this point shifts towards the walls of the column which results in decrease in liquid recirculation. Due to high momentum of liquid velocity, gas phase creates less circulation in the column. In the gas holdup profiles, average gas holdup decreases with increasing liquid velocity. High velocity of the liquid phase reduces the residence time of bubbles in the reactor, which results in decreasing the gas holdup. In Fig. 6 the gas holdup profiles shift down with increasing liquid velocity. High momentum of liquid phase induces high rise velocities for the bubbles which results a decrease in gas holdup. The peak in the profile shifts towards the wall with increase in liquid velocity. This says that the liquid circulation has been decreases in the annulus reason.

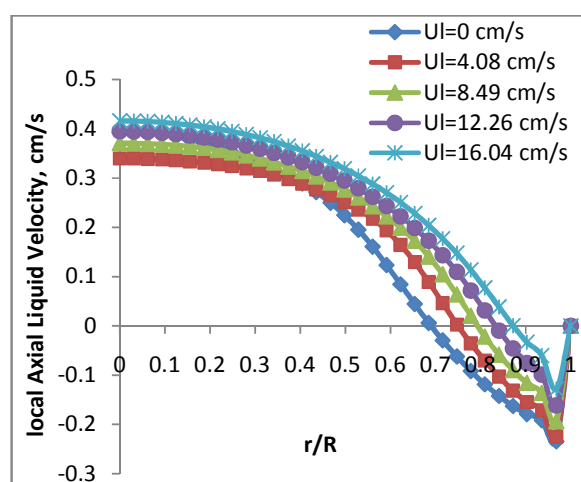


Fig. 5 (a) Radial distribution of axial liquid velocity profiles for superficial gas velocities $U_g = 4.53$ cm/s

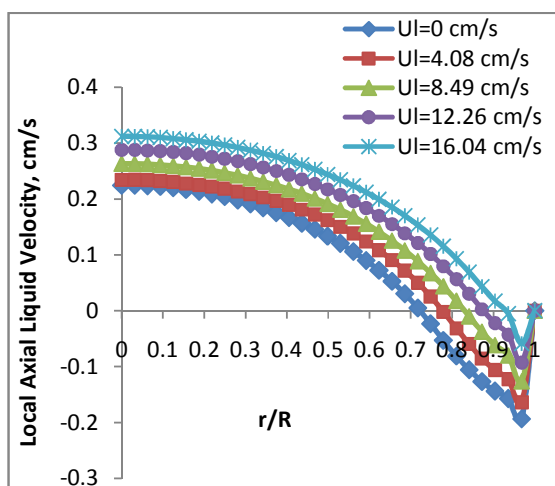


Fig. 5 (b) Radial distribution of axial liquid velocity profiles for superficial gas velocities $U_g=10.19$ cm/s

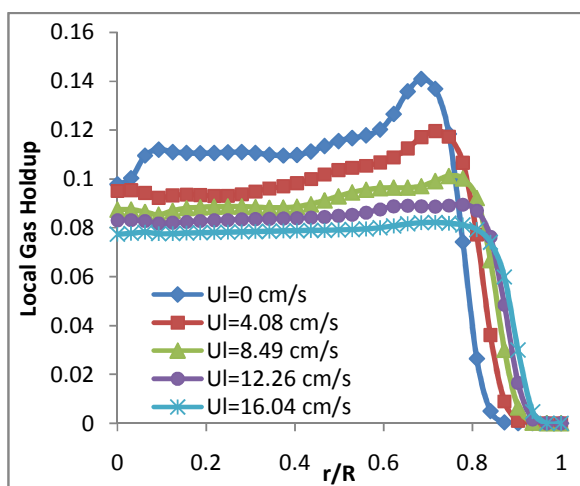


Fig. 6 (a) Radial distribution of Gas Holdup profiles for $U_g=4.53$ cm/s

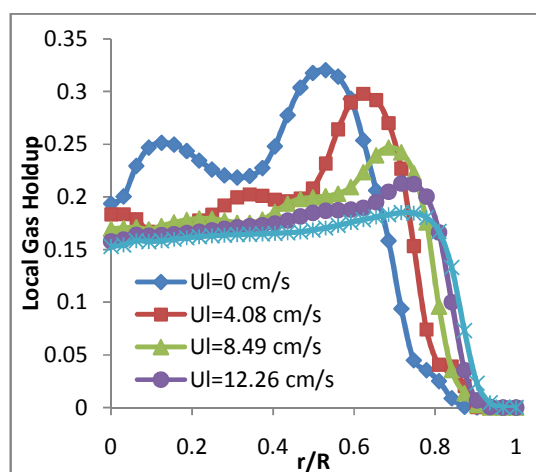


Fig. 6 (b) Radial distribution of Gas Holdup profiles for $U_g=10.19$ cm/s

B. Three-Phase as pseudo two phase Simulation

In three-phase gas-liquid-solid slurry systems, the suspension of solids in the liquid is usually modeled as a single pseudo-homogeneous slurry phase [25]-[28]. Within the slurry phase, the solids velocity is assumed to be equal to the liquid velocity. Hence, slurry bubble column reactors are most often modeled as two-phase gas-slurry systems. Pseudo slurry assumption is probably reasonable because, the mean size of solid particles that has been used in the slurry bubble column is below $50\ \mu\text{m}$ [26]. In the present case, solid-liquid phase was treated as a single phase with average density and viscosity. The viscosity was calculated using

$$\mu_p = \mu_l \left(1 + \varepsilon_s \frac{\rho_s - \rho_l}{\rho_s} \right) (1 - \varepsilon_s)^{-2.59} \quad (11)$$

where μ_p is the viscosity of primary (slurry) phase [29]. The density was calculated using

$$\rho_s = \frac{\rho_l \varepsilon_l + \rho_s \varepsilon_s}{\varepsilon_l + \varepsilon_s} \quad (12)$$

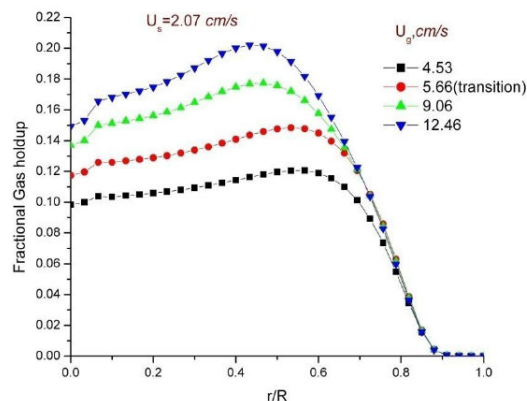


Fig. 7 Radial distribution of total gas hold-up for $U_s=2.07$ cm/s at solid concentration 9.0 wt% height of column $H/D = 5$

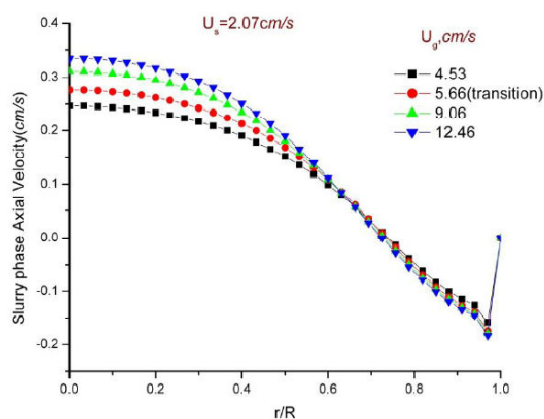


Fig. 8 Axial liquid velocity distribution for $U_s = 2.07$ cm/s at solid concentration 9.0 wt% height of column $H/D = 5$

As shown in Fig 7 & 8, the trend is the same as two phase flow. The liquid recirculation occurs at $r/R = 0.7$. The gas holdup increases with increase in the gas velocity. The peak of the gas holdup profile shifts towards the centre of the column, when superficial gas velocity is increased.

V.CONCLUSION

The Euler-Euler simulations for two phase bubble column have been performed and compared with the experimental results. Uniform bubble size (5mm) was assumed at the sparger inlet to ensure uniform bubble size distribution. The liquid recirculation in the column has been shown using the axial liquid velocity profiles. The circulation decreases with increase in the liquid velocity. As the liquid velocity increases, the gas holdup decreases for a fixed gas velocity due to decrease in liquid recirculation in the column. Hence by increasing gas phase velocity, the gas holdup can be increased for higher liquid velocities. The radial gas holdup distribution has also been predicted using the simulation. Pseudo two phase simulations could be used to model the three phase flow with low solid loadings.

ACKNOWLEDGMENT

The authors acknowledge the research grant support provided by Chevron, USA; Advanced Refining Technologies (ART), USA and Hindustan Petroleum Corporation Limited (HPCL), India.

REFERENCES

- [1] J. Schallenberg, J. H. Enß, D. C. Hempel, "The important role of local dispersed phase holdups for the calculation of three-phase bubble columns," *Chemical Engineering Science*, vol. 60, pp. 6027–6033, 2005.
- [2] W. D. Deckwer, "Bubble Column Reactors," *Wiley, New York*, 1992.
- [3] Y. T. Shah, S. P. Godbole, W. D. Deckwer, "Design parameters estimations for bubble column reactors," *AIChE Journal*, vol. 28, pp. 353–379, 1982.
- [4] H. Li, A. Prakash, "Heat transfer and hydrodynamics in a three-phase slurry bubble column" *Ind Eng Chem Res*, vol. 36, pp. 4688–4694, 1997.
- [5] W. D. Deckwer, A. Schumpe, "Improved tools for bubble column reactor design and scale-up," *Chemical Engineering Science*, vol. 48, pp. 889–911, 1993.
- [6] X. Luo, D. J. Lee, R. Lau, G. Yang, L. Fan, "Maximum stable bubble size and gas holdup in high-pressure slurry bubble columns," *AIChE Journal*, vol. 45 pp. 665–685, 1999.
- [7] G. Eigenberger, A. Sokolichin, "Applicability of the standard $k-\epsilon$ turbulence model to the dynamic simulation of bubble columns. part i. detailed numerical simulations," *Chemical Engineering Science*, vol. 54, pp. 2273–2284, 1999.
- [8] V. V. Ranade, V. V. Buwa, "Characterization of dynamics of gas-liquid flows in rectangular bubble columns," *AIChE Journal*, vol. 50, pp. 2394–2407, 2004.
- [9] A. Sokolichin, G. Eigenberger, O. Borchers, C. Busch, "Applicability of the standard k-epsilon turbulence model to the dynamic simulation of bubble columns. part ii. Comparison of detailed experiments and flow simulations," *Chemical Engineering Science*, vol. 54, pp. 5927–5935, 1999.
- [10] K. Bech, "Dynamic simulation of a 2d bubble column," *Chemical Engineering Science*, vol. 60, pp. 5294–5304, 2005.
- [11] N. Gilbert, H.G. Wagner, D. Peger, S. Gomes, "Hydrodynamic simulations of laboratory scale bubble columns fundamental studies of the eulerian-eulerian modeling approach," *Chemical Engineering Science*, vol. 54, pp. 5091–5099, 1999.
- [12] M. I. Urseanu R. Krishna, J.M. van Baten, "Three-phase eulerian simulations of bubble column reactors operating in the churn-turbulent regime: a scale up strategy," *Chemical Engineering Science*, vol. 55, pp. 3275–3286, 2000.
- [13] M. Chang, Y. Pan, M. P. Dudukovic, "Dynamic simulation of bubbly flow in bubble columns," *Chemical Engineering Science*, vol. 54, pp. 2481–2499, 1999.
- [14] V. V. Ranade, V. V. Buwa, D.S. Deo, "Eulerianlagrangian simulations of unsteady gasliquid flows in bubble columns" *Int. J. Multiphase Flow*, vol. 32, pp. 864–885, 2006.
- [15] J. A. M. Kuipers, W. P. M. van Swaaij, E. Delnoij, F. A. Lammers, "Dynamic simulation of dispersed gas-liquid two-phase flow using a discrete bubble model," *Chemical Engineering Science*, vol. 52, pp. 1429–1458, 1997.
- [16] J. A. M. Kuipers, D. Darmana, N. G. Deen, "Detailed modeling of hydrodynamics, mass transfer and chemical reactions in a bubble column using a discrete bubble model," *Chemical Engineering Science*, vol. 60, pp. 3383–3404, 2005.
- [17] A. Lobbert, A. Lapin, "Numerical simulation of the dynamics of two-phase gas-liquid flows in bubble columns," *Chemical Engineering Science*, vol. 49, pp.3661–3674, 1994.
- [18] O. Simonin, R. F. Mudde, "Two- and three-dimensional simulations of a bubble plume using a two-fluid model," *Chemical Engineering Science*, vol. 54, pp. 5061–5099, 1999.
- [19] A. Lapin A. Liibbert A. Sokolichin, G. Eigenberger, "Dynamic numerical simulation of gas-liquid two-phase flows euler/euler Vs euler/lagrange," *Chemical Engineering Science*, vol. 49, pp. 3661–3674, 1997.
- [20] H. D. Mandelson, "The prediction of bubble terminal velocities from wave theory," *AIChE Journal*, vol. 13, pp. 250, 1967.
- [21] J. P. Vandoormaai, G. D. Raithby, "Enhancements of the SIMPLE Method for Predicting Incompressible Fluid Flows," *Numer. Heat Transfer*, vol. 7, pp. 147–163, 1984.
- [22] Z. Naumann, L. Schiller, "A drag coefficient correlation," *Z. Ver Deutsch. Ing.*, vol. 77, pp. 318–323, 1935.
- [23] D. Z. Zhang, W. B. Vanderheyden, "The effects of meso-scale structures on dispersed two-phase flows and their closures in dilute suspensions," *International Journal of Multiphase Flow*, vol. 28, pp. 805, 2002.
- [24] A. Tomiyama, H. Tamai, I. Zun, and S. Hosokawa, "Transverse migration of single bubbles in simple shear flows," *Chemical Engineering Science*, vol. 57, pp. 1849–1858, 2002.
- [25] R. Krishna, J.M. van Baten, J. Ellenberger, "Scale-up strategy for bubble column slurry reactors using cfd simulations," *Catalysis Today*, vol. 79–80, pp. 259–265, 2003.
- [26] M. P. Dudukovic, N. Rados, M. H. Al-Dahhan, "Dynamic modelling of slurry bubble column reactors," *Ind. Eng. Chem. Res.*, vol. 44, pp. 6086–6094, 2005.
- [27] F. Zdravistich, A. A. Troshko, "Cfd modelling of slurry bubble column reactors for fisher-tropsch synthesis," *Chemical Engineering Science*, vol. 64, pp. 1892–1903, 2009.
- [28] W. Feng, J. Wen, J. Fan, Q. Yuan, X. Jia, Y. Sun, "Local hydrodynamics of gas-liquid-nano particles three-phase fluidization," *Chemical Engineering Science*, vol. 60, pp. 6887–6898, 2005.
- [29] G. Hillmer, L. Weismantel, H. Halfmann, "Investigations and modelling of slurry bubble columns," *Chemical Engineering Science*, vol. 49, pp. 837–843, 1993.